ELSEVIER

Journal of Nuclear Materials 258–263 (1998) 740–744

journal of nuclear materials

Thermal stability and chemical erosion of the silicon doped CFC material NS31

M. Balden [a,*], J. Roth [a], C.H. Wu [b]

[a] *Max-Planck-Institut für Plasmaphysik, EURATOM Association, postfach 1533, Boltzmannstr. 2, D-85740 Garching bei Munchen, Germany*

[b] *NET Team, Max-Planck-Institut für Plasmaphysik, EURATOM Association, Boltzmannstr. 2, D-85748 Garching, Germany*

Abstract

The thermal stability of the 8–10 at.% Si doped 3D CFC material NS31 was investigated using scanning electron microscopy (SEM) and ion beam analysis. Total erosion yields and CD_4 production yields were determined by bombarding with monoenergetic deuterium ions. During heating to 1800 K SiC crystallites of a few μm size are created on the surface. A Si depletion at the surface and an enrichment layer (20–50 at.% Si) beneath the surface of about 5–10 μm thickness were observed. They are explained by the distribution of the crystallites of μm size and the evaporation of Si from the surface. After heating a NS31 mock-up tile to temperatures above 2300 K in a power load test, the Si concentration in a surface layer of more than 5 μm thickness drops below 3 at.% Si. The chemical erosion is reduced for the initial and heated samples by a factor of 2–3 compared to pure graphite. NS31 shows sputtering yields between those of graphite and silicon carbide depending on the Si concentration of the individual surface. © 1998 Elsevier Science B.V. All rights reserved.

1. Introduction

The successful operation of future fusion reactors will depend on the ability of plasma facing components to handle enormous particle and power loading [1,2]. These loadings differ significantly with the position of the component in the fusion chamber [2,3]. The component lifetime [4] and the contamination of the plasma will be determined by the erosion mechanisms (e.g. sputtering or evaporation) and their rates [5], as well as by the transport and re-deposition of eroded material [6]. Off-normal conditions (e.g. disruptions) and slow high power transients cause mechanical stress and extreme heat loads [1]. Therefore, they have to be taken into account as additional requirements [4]. So, for ITER the use of a combination of carbon, beryllium, and tungsten is planned [1,7]: Be for the main wall, W for the baffles and divertor walls, and C for the divertor target plates.

The disadvantage of pure carbon materials is the chemical reactivity with hydrogen and oxygen and the large amount of tritium retained in re-deposited carbon layers. The chemical reactivity could be reduced by dopants, e.g. silicon, boron, or titanium [8,9]. The distribution of the dopant in the surface affects the erosion behaviour of the material. For the tritium retention, three different aspects are important: trapped tritium in the implantation zone, migration of tritium into the bulk of the plasma facing materials, and co-deposition of tritium in the re-deposited material. All three are effected in a different way by the dopants and by the microstructure of the material.

Normally the thermal conductivity is related to the microstructure of the materials and the perfection of the crystal structure. Therefore, in carbon materials dopants reduce in general the thermal conductivity. However, in co-operation of Societe Europeenne de Propulsion (SEP), France, and NET Team, a silicon doped carbon fibre composite (CFC) has been developed with an optimized thermal conductivity. This 3D CFC material reaches a thermal conductivity of 300 W/mK at room temperature in one particular direction [10] and has been recommended as the ITER reference material [11].

* Corresponding author. Tel.: +49 89 3299 1262; fax: +49 89 3299 1149; e-mail: balden@ipp.mpg.de.

0022-3115/98/$19.00 © 1998 Elsevier Science B.V. All rights reserved.
PII: S0022-3115(98)00254-2

At elevated temperatures the evaporation of dopants is expected. Due to the evaporation the concentrations near the surface [12,13] (and perhaps in the bulk) and the microstructure would be changed. Therefore, it may influence the erosion yield due to ion bombardment and the tritium retention in the implantation zone, bulk, and co-deposited layers.

The present paper deals with the consequences of a heat treatment to the material NS31. The morphology, the dopant distribution, the total erosion yield, and the amount of retained deuterium after implantation before and after heating to 1800 K were investigated. Also mock-up flat tiles of NS31 after power load tests were studied.

2. Experimental

The 3D CFC material NS31 from the manufacturer SEP was used for the experiments. The manufacturing procedures are described elsewhere [14]. This 3D CFC is specified with an average silicon concentration of 8–10 at.%, a density of 2.0 g/cm^3 and a porosity around 5%.

A block of NS31 was mechanically cut into small plates (usually $12 \times 15 \times 1$ mm^3) and cleaned in an ultrasonic bath. Some of these initial samples were heated in vacuum at 1800 K for 2 h. In order to obtain information on the bulk of heated NS31 (1 mm beneath surface), some of the heated samples were cut once more. These faces are called 'cut' faces in the paper.

A second set of samples was obtained by cutting a mock-up flat tile of NS31, which was exposed to 18 MW/m^2 power load for 1000 pulses of about 10 s in the 200 kW FE200 at Framatome in LeCreusot, France [15]. During the loading the material reaches a temperature above 2300 K.

In order to get a view of the surface topography, scanning electron microscopy (SEM) was performed. Coupled with the topographic image from the secondary electrons the electron induced X-ray emission (EIXE) yields information on the composition of the material from throughout the penetration depth of the electron beam of about 1–3 μm.

The silicon distribution and depth profile near the surface was determined using backscattering spectrometry of 2.0 MeV ^{4}He ions and 2.5 MeV protons with information depth of about 1 and 20μm, respectively. The ion beam hits the target at normal incidence. The scattering angle was 165°. The size of the analysing spot was about 0.5–1.5 mm^2. To specify the impurity content proton induced X-ray emission (PIXE) was performed using 1.5 MeV protons.

For the erosion measurements the Garching high current ion source [16] was adjusted to produce 3 or 6 keV mass separated ions, mostly D_3^+ ions. These ions were slowed down by biasing the target to the chosen impact energy. The bombarded spots had sizes between 0.5 and 0.8 cm^2 depending on the impact energy. An ion current between 35 and 100 μA was used corresponding to fluxes of about $1–4 \times 10^{15}$ D/cm^2/s. The sputtering yield was determined by measuring the weight loss and the total ion charge. The amount of neutrals in the beam, not decelerated by the target bias was determined by the sputtering yield of Au at 60 eV impact energy. This ion energy is below the threshold for physical sputtering of Au. Therefore, the measured yield can be assigned to neutral deuterium atoms, which provides a flux of neutrals of about 3% of the ion flux. The neutrals in the beam could be reduced below the detection limit of about 0.3% by a match of a magnetic and an additional electrostatic deflection of the beam. The chemical erosion of pure graphite was not measurably influenced by the neutrals. As a result synergistic effects due to the chemical erosion could be excluded [17].

In order to determine the chemical part of erosion the CD_4 production versus the target temperature was monitored and compared to that of pure carbon (pyrolytic graphite (HPG) from Union Carbide, USA). During the bombardment the temperature was increased in steps and held for 6 min to ensure steady state conditions. Degassing experiments after D_3^+ implantation were performed using thermal desorption spectroscopy (TDS) up to 1450 K with about 6 K/s linear heating rate. Information on the amount of retained D was obtained and compared to pyrolytic graphite.

3. Results

The 3D CFC NS31 shows a strong anisotropy on the thermal conductivity. However, no dependence of the Si concentration and the sputtering yield on the orientation of the sample surface with respect to the high thermal conductivity direction was observable in all our measurements.

3.1. Initial NS31

In SEM, four different areas of 0.01–1 mm^2 size could be characterized on the surface of initial NS31. These areas consist of pure graphite, big crystallites (30 μm) of Si or SiC, thin carbon fibres (6 μm diameter), and thick carbon fibres (30 μm diameter) with a smooth coating of Si or SiC visible in holes due to manufacturing procedure. Because of the fibre structure, the material NS31 is inhomogeneous in dimension of millimetres. Due to ion bombardment strong erosion profiles are created at the graphite areas with structures beneath 1 μm, the Si or SiC crystallites are rounded, and on all thick Si or SiC covered fibres crystallites (4–12 μm) have been grown.

The spot of the analysing ion beam is too small to average over the lateral inhomogeneity and to obtain a

representative spectrum for a sample face. Therefore, for each face a series of spectra at different positions were averaged. In Fig. 1 the spectra for many initial faces are averaged for 2.0 MeV ^{4}He and for one initial face for 2.5 MeV proton backscattering. The signal at the Si and C edge results from backscattering from surface atoms. The energy scale is an equivalent for a depth scale for each element separately; lower backscattering energies mean increasing the depth. For comparison a simulated spectrum using the program SIMNRA [18] of a homogeneous mixture of 8 at.% Si and 92 at.% C is ploted in Fig. 1(a), which agrees well with the average spectrum of the initial face. The shape of each single measured spectra for the initial surface could be reproduced by a homogeneous Si distribution in depth with laterally varying the Si concentration between 0 and 20 at.% Si.

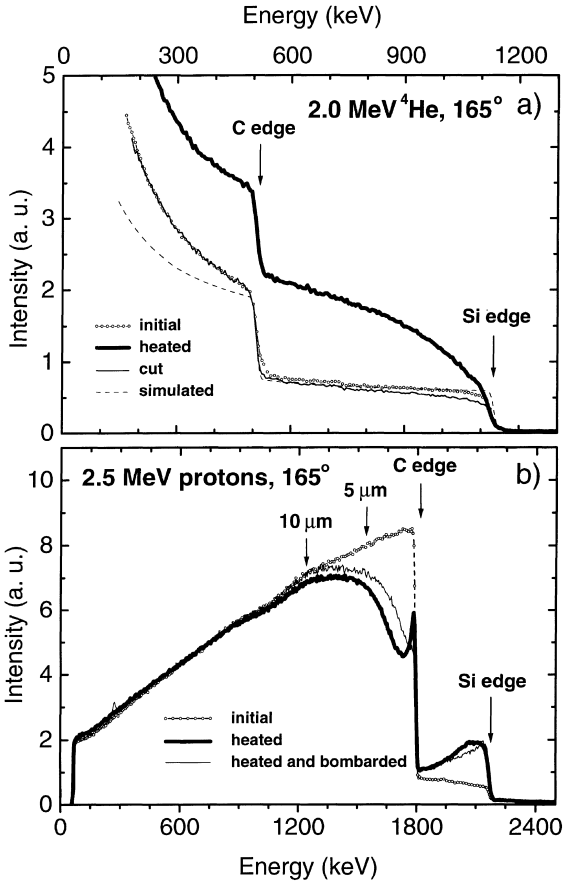

Fig. 1. (a) Backscattering spectra of 2.0 MeV ^{4}He averaged over several initial (dotted), heated (thick line), and 'cut' faces (thin line). The dashed line represents a simulated spectrum of a homogeneous mixture of 8 at.% Si and 92 at.% C. (b) Average spectra measured with 2.5 MeV protons of an initial (dotted), a heated (thick line), and a heated and bombarded face (thin line). The energies corresponding to the depth of about 5 and 10 μm for the carbon signal of the initial face are marked.

Averaging over one face the variation is reduced to 5–12 at.% Si.

For the determination of the sputtering yield based on weight loss measurements, the composition of the sputtered material has to be taken into account: It can be assumed that at high fluences the composition of eroded material is equal to the bulk composition and that this steady state is reached in our measurements. For initial faces 10 at.% Si in carbon were used.

The temperature dependence of the sputtering yield of pyrolytic graphite and NS31 due to the dominant chemical erosion processes – the thermally activated hydrocarbon emission (Y_{therm}) [19,20] – was measured. The maximum for both, graphite and NS31, was found at the same temperatures, at about 850 K for 200 eV deuterium and at about 700 K for 30 eV deuterium. To relate the yield of NS31 to those of graphite and silicon carbide [17,19,21], the measured yields are plotted in Fig. 2 versus the impact energy. The measured yields are between the yield of graphite and silicon carbide. At around 800 K a reduction of a factor about 2 compared to graphite was obtained throughout the energy range. At 300 K, below 100 eV the kinetic ejection of surface hydrocarbon complexes from a collisional energy transfer (Y_{surf}) exceeds the unavoidable physical sputtering [19,20], which dominates the yield above 100 eV. Also this chemical erosion is reduced. By measuring the chemical erosion directly from the CD_4 production of 1 keV deuterium, the results of the weight loss measurements (temperature dependence and reduction) were confirmed.

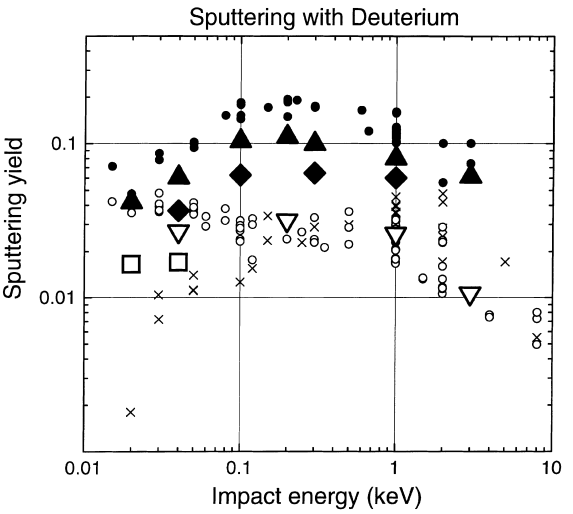

Fig. 2. Sputtering yield data of pure graphite (circles) [17,19], of SiC (crosses) [21], of initial faces (triangles), and heated faces of NS31 (squares/diamonds) for perpendicular incidence of deuterium versus impact energy. Open data points were measured at 300 K, filled ones around 800 K with fluxes of around 1–4×10^{15} D/cm^2/s.

In order to obtain information about the amount of retained deuterium after implantation, TDS measurements were performed. The shape of the TDS spectra of initial NS31 and pyrolytic graphite looks similar. The contribution of the silicon as inferred from measurements on SiC [22] is too small to be visible. The amount of retained D in NS31 did not completely saturate with fluence, a well known behaviour of porous pure and doped graphites [22,23]. This could be interpreted as the migration of deuterium into the bulk along grain boundaries and trapping beyond the implantation zone [24]. More details to this topic can be found in [22].

3.2. Heated NS31

Due to the first heating to 1800 K for 2 h, a weight loss of about 1–5% of 0.3 g samples has been observed together with a deposition of evaporated silicon on the walls of the heating chamber. During a second heat treatment the relative weight loss is less than 6×10^{-4}.

3.2.1. Surface of heated NS31

From the four different areas of initial faces visible in SEM, only the thick fibres are not modified by the heat treatment. They stay smooth. The other areas are sprinkled with small crystallites of Si or SiC (1–8 μm). After additional D_3^+ bombardment the concentration of the small crystallites was increased. Rounded Si or SiC crystallites and strong erosion profiles in the graphite inbetween the crystallites are visible. Every thick fibre is covered completely with rounded crystallites (4–12 μm).

In Fig. 1(a), the average backscattering spectrum of several heated faces shows an increasing Si intensity below the Si edge. Such a shape of a 2.0 MeV ^{4}He backscattering spectrum can be explained by a Si profile starting with a silicon depletion near the surface and enrichment with depths. An increasing Si concentration with depth is also indicated by the EIXE measurements, where the intensity of the silicon EIXE signal on a heated face decreases with decreasing penetration depth (decreasing electron beam energy), while it was constant on initial and 'cut' faces. By iterating the concentration and depth profile in the program SIMNRA [18], the backscattered spectra are simulated. To obtain a depth scale for the profiles an atomic density for NS31 of 0.9×10^{23} at./cm^3 was used neglecting changes in density. In a depth of around 0.5 μm, for some heated faces a big variation between 0 and 40 at.% Si at different positions was observed. For some other faces the variation was only between 40 and 50 at.% Si.

In the backscattering spectra of 2.5 MeV protons (e.g. in Fig. 1(b)), the Si depletion zone at the heated surface produces a narrow peak at the carbon edge. The dip in the carbon signal at around 1700 keV and the increase of the signal below the Si edge in comparison with a spectrum of an initial face characterize the Si enriched layer. From the comparison with simulated spectra, the thickness of the enrichment layer could be determined. It varies for the different face between around 5–10 μm. By deuterium bombardment the altered layer can be partly removed, as the missing peak at the C edge and the shift of the dip in the carbon signal and of the Si peak indicate (Fig. 1(b)).

The sputtering yields are averaged values over the removed part of the Si profile. By measuring the CD_4 production of a freshly heated surface and after removing parts of the enrichment layer, it could be clearly shown that the chemical erosion decreases with increasing Si concentration. For all impact energies the measured total sputtering yield for the heated surfaces is lower than for the initial NS31 (Fig. 2). A reduction of a factor 3 compared to graphite is reached.

In the TDS measurements no differences between heated surfaces and initial faces were observed, except that the shape of the TDS spectra shows an indication for a higher silicon contribution of the heated surfaces. The amount of retained D is the same.

3.2.2. Bulk of heated NS31

A freshly cut face of a heated sample looks like an initial face with all four features clearly visible in SEM. The only noticeable change due to the heat treatment is the roughening of the coating of the thick fibres with structures below 1 μm size. In the ion beam analysis the lateral distribution of the silicon, the shape of the single measured spectra, and the average spectrum of several 'cut' faces (Fig. 1(a)) could not be distinct from those of the initial faces. Also in the determination of the sputtering yield no difference was observable.

Heating a 'cut' face a second time to 1800 K for 2 h, an enrichment layer does not occur and only the depletion zone is created. Such a depletion is a well known behaviour of Si doped graphites due to evaporation of Si [12,13].

3.3. Mock-up tiles

3.3.1. Surface of mock-up tiles

In SEM, the surface of the mock-up tiles shows strong erosion profiles with structure of a size of around 1 μm, also on the thick carbon fibres. Due to the smallness of the structures it is difficult to distinguish between graphite areas and crystallites. With EIXE areas of pure carbon could be found, as well as areas with high amounts of Si. But additional a tungsten signal was observed in EIXE as well as in PIXE. Tungsten pellets could not be resolved on the surface in SEM. Due to the high mass of W, these contaminations lead to disturbing signals in the backscattering spectra extending to the energies of the Si edge and below. So, if the whole signal just above the C edge is attributed to Si, the Si concentration could be estimated to below 3 at.% in the

surface layer of at least 5 μm. Tungsten concentrations up to 4 at.% W were observed at the surface with decreasing concentration with increasing depth. The tungsten on the mock-up tiles originates from neighbouring W mock-up's during the heat load test. Due to the high W contamination no sputtering and TDS measurements of the mock-up tiles were performed.

3.3.2. Bulk of mock-up tiles

In contrast to the surface, for the bulk of the mock-up tiles the ion beam analysis and REM do not provide any difference to initial or 'cut' faces. So, the results of the initial faces could relate to the bulk of the mock-up tiles.

4. Discussion

The silicon concentration at the surface of the as-received NS31 is altered after heating to elevated temperatures. The observed results of SEM and ion beam analysis imply that during the heat treatment to 1800 K for 2 h, free silicon segregates to the surface and enriches a layer of 5–10 μm thickness. Silicon carbide is formed during this process. With extending heating time, a fraction of the Si from the surfaces of the SiC crystallites evaporates. The observed profiles reflect the average over the distribution of the crystallites of μm size and the depletion of surface in Si. The Si concentration in the enrichment layer depends on the non-uniform characteristics of the received NS31. In particular, the distribution of free Si causes different degrees of enrichment. It is interesting to note, that no further Si segregation has been observed in NS31 after additional heat treatments.

During the high heat load (18 MW/m^2) of mock-up tiles, surface temperatures up to 2300 K have been reached. A rapid evaporation of Si caused a depletion of Si in a surface layer of more than 5 μm thickness.

The distribution of the SiC crystallites influences the sputtering yield. A comparison of initial, heated, and heated/bombarded faces shows a reduction of the sputtering yield increases with increasing Si concentration. Overall, a reduction by a factor of about 3 compared to graphite has been found for heated/bombarded NS31 samples. In addition, a reduction of the chemical erosion due to the flux and energy dependence should be kept in mind [19,20,25].

Acknowledgements

The authors would like to thank J. Gruber (Institut Dr. Ing. H. Klingele, Adelgundenstr. 8, 80538 München, Germany), S. Bassen, W. Ottenberger, and H. Plank (IPP) for the experimental performance and assistance and P. Chappuis (CEA) and G. Vieider (NET) for useful discussion.

References

[1] R. Parker, G. Janeschitz, H.D. Pacher, D. Post, S. Chiocchio, G. Federici, P. Ladd, ITER joint central team and home teams, J. Nucl. Mater. 241–243 (1997) 1.
[2] G. Janeschitz, K. Borrass, G. Federici, Y. Igitkhanov, A. Kukushin, J. Nucl. Mater. 220–222 (1995) 73.
[3] H. Verbeek, J. Stober, D.P. Coster, R. Schneider, 24th EPS Conference on Controlled Fusion and Plasma Physics, vol. 21A of Europhysics Conference Abstracts, 1997, p. 1457.
[4] H.D. Pacher, I. Smid, G. Federici, Y. Igitkhanov, G. Janeschitz, R. Raffray, G. Vieider, J. Nucl. Mater. 241–243 (1997) 255.
[5] W.O. Hofer, J. Roth, Physical Processes of the Interaction of Fusion Plasmas with Solids, Academic Press, New York, 1996.
[6] M. Mayer, R. Behrisch, P. Andrew, A.T. Peacock, J. Nucl. Mater. 241–243 (1997) 469.
[7] C.H. Wu, U. Mszanowski, J. Nucl. Mater. 218 (1995) 293.
[8] J. Roth, H. Plank, R. Schwörer, Physica Scripta T64 (1996) 67.
[9] H. Plank, R. Schwörer, J. Roth, Surf. Coat. Technol. 83 (1996) 93.
[10] C.H. Wu, C. Alessandrini, P. Bonal, A. Caso, H. Grote, R. Moormann, A. Perujo, M. Balden, H. Werle, G. Vieider, Fusion Technology Special Issue (1996) 327.
[11] ITER Document, IDoMS Nr. G17 MI22 97-05-21 F1, 1997.
[12] J. Roth, J. Bohdansky, J.B. Roberto, J. Nucl. Mater. 128–129 (1984) 534.
[13] I. Fujita, H. Hirohata, T. Hino, T. Yamashima, Y. Kubota, N. Noda, O. Motojima, T. Sogabe, T. Matsuda, K. Kuroda, J. Nucl. Mater. 241–243 (1997) 1185.
[14] SEP, Final report NS31, Tech. rep., France, 1996.
[15] G. Vieider et al., Overview of the EU small scale mock-up tests for ITER high heat flux components, Proceedings of 4th ISFNT, Tokyo, 1997.
[16] W. Eckstein, C. Garcá-Rosales, J. Roth, W. Ottenberger, Sputtering data, Tech. Rep. IPP 9/82, Max-Planck-Institut für Plasmaphysik, Garching, 1993.
[17] M. Balden, J. Roth, Unpublished data (in preparation for publishing).
[18] M. Mayer, SIMNRA User's Guide, Tech. Rep. IPP 9/113, Max-Planck-Institut für Plasmaphysik, Garching, 1997.
[19] J. Roth, C. Garcá-Rosales, Nucl. Fusion 36 (1996) 1647.
[20] J. Roth, C. Garcá-Rosales, Nucl. Fusion 37 (1997) 897.
[21] H. Plank, R. Schwörer, J. Roth, Nucl. Instr. and Meth. B 111 (1996) 63.
[22] M. Mayer, M. Balden, R. Behrisch, J. Nucl. Mater. 252 (1998) 55.
[23] A.A. Haasz, J.W. Davis, J. Nucl. Mater. 209 (1994) 155.
[24] A.A. Haasz, P. Franzen, J.W. Davis, S. Chiu, C.S. Pitcher, J. Appl. Phys. 77 (1995) 66.
[25] H. Grote, W. Bohmeyer, H.-D. Reiner, T. Fuchs, P. Kornejew, J. Steinbrink, J. Nucl. Mater. 241–243 (1997) 1152.